Proceedings of the 39th Chinese Control Conference
July 27-29, 2020, Shenyang, China

Design of UGV Trajectory Tracking Controller in UGV-UAV Cooperation

Qize Wu[1], Juntong Qi[1], Chong Wu[1], Mingming Wang[1]

1. School of Electrical and Information Engineering Tianjin University, Tianjin 300072, China
E-mail: wuqize@tju.edu.cn

Abstract: In the leader-following formation of unmanned aerial vehicles (UAVs) and unmanned ground vehicles (UGVs), when the UAV moves in the direction of the UGV motion constraint, traditional PID controller has a series problem, such as poor stability, large overshot. These problems affect the formation maintenance. In order to solve these problems, the following research is carried out. Firstly, the kinematic model and dynamical model of the UGV are analyzed. Secondly, an improved expert PID target tracking control algorithm is proposed which adjusts PID parameters online according to the knowledge base to improve response speed and stability. To build the knowledge base, lots of experiments are carried out. The problem of sudden change of the control amount when switching parameters is solved by the cubic function fitting smoothing. Finally, a UAV-UGV indoor experimental platform is built to verify the effectiveness of the proposed method, and the experimental result shows that the improved expert PID based target tracking control algorithm has superior response speed and stability.

Key Words: UAV-UGV, Target tracking, Expert PID, Cubic function fitting

1 Introduction

With the advent of artificial intelligence technology, many researchers are committed to the research of UAVs and UGVs. UAVs can quickly detect a large area, however, due to the minimum limit of height and speed, UAVs are greatly limited in detecting ground targets. UGVs can detect ground targets at a close range, but are limited by speed, terrain and field of view. The UAV-UGV cooperation can combine advantages of UAVs and UGVs to accomplish tasks, such as topographic survey, logistics and transportation, target tracking that are unable to accomplish by UAVs or UGVs.

Considering different application scenarios, researchers have done lots of work. Chen J proposed a decomposition-based method for target tracking to reduce the computational complexity and achieve good results [1]. Antun Ivanovic proposed a cooperative UAV-UGV team. The UAV was used for long-range detection and the UGV was used as a landing platform. The overall system framework was proposed, including motion planning and complex task assignment [2]. Lucas Vago Santana proposed a heterogeneous leader-follower formation control structure, and a centralized control structure was used. A centralized controller was used to control the UAV-UGV formation and the effectiveness of the method was verified through experiments [3].

Currently, because UAVs had greater maneuverability, when the UAV-UGV cooperate work, researchers used UAVs to track UGVs. The computer vision technology was used to identify targets, and appropriate control algorithms were used to achieve UAVs tracking UGVs [4-6]. In the target tracking control of the UAV, compensation based on multiple sensors was needed and the sensor data was integrated to accurately estimate the attitude information. Then, the path planning algorithm was designed to target tracking according to the constraints of the quadrotor dynamics [7]. Abderrahmane Lakas proposed a UAV-UGV cooperative navigation framework. The UAV was used to collect environmental information and then guide the UGV to move to the target point [8]. This paper developed a series of control rules, aiming at improving computational efficiency without compromising the performance. In some application scenarios, it is difficult for UAVs to achieve precise control, such as harsh environments or height restrictions. On the contrary, the UGV can perform stable control in complex environments. Jun Ni proposed a robust controller for UGV path tracking, and the effectiveness was verified through experiments [9]. Oscar Barrero proposed a positioning system based on EKF and kinematic model, and a PID-based trajectory tracking controller was used [10]. However, the PID controller was affected by system parameters and environmental factors, the control algorithm needs to be further optimized. Sen Zhu designed a UGV based on hybrid structure and the layered control structure was used to realize the requirement of actual environment [11]. The pure pursuit algorithm used the geometry to calculate the arc radius and selected the appropriate look-ahead distance that the UGV required. Due to its convenience and satisfactory response, the pure pursuit algorithm was widely used in the path tracking field [12-13]. Haytham A proposed a GA-tuned-PID controller to improve steering stability by reducing the error between the vehicle of heading and the target point. When the angle changes greatly, further optimization of the path tracking algorithm was needed [14]. Luo Z proposed an expert PID controller to solve the problem that the traditional PID parameters cannot be adjusted dynamically. This method combined professional knowledge and experience to adjust the parameters in real time to achieve better control effects [15]. However, the discontinuous change of the parameters led to a sudden change in the control amount.

The remaining structure of this paper is as follows. First, this paper analyzes the kinematic model and dynamical model of UGVs in Section 2. Second, the improved expert PID target tracking control algorithm is introduced in Section 3. Third, the construction of UAV-UGV platform is completed in Section 4. Then, the experimental results are

analyzed in Section 5. Finally, the research completed and future improvements is summarized in Section 6.

2 Model Analysis of UGV

2.1 Dynamic Model Establishment

The UGV is a typical non-holonomic constraint system, so establishing a correct mathematical model is the basis of the UGV motion control. According to the demand, the UGV adopts two-wheel differential drive. To simplify the analysis, the following assumptions are made:

- The UGV is a uniform and symmetrical rigid body without internal forces and deformation.
- During motion, the UGV does not slip.
- The origin of the body coordinate system coincides with the center of mass.

The non-holonomic constraints imposed by a non-holonomic constraint system are in the form of non-integrable differential equations, which are converted to the non-integrable Pfaffian constraint.

$$\Re(\xi)\bullet\dot{\xi} \tag{1}$$

where $\Re(\xi) \in R^{m\times n}$ is the coefficient matrix of the generalized coordinate of the system ($m>n$). $\xi \in R^n$ is the generalized coordinate vector of the system. The motion of the UGV is a non-holonomic constrained motion and the formula is as follows:

$$\Re(\xi)\bullet\dot{\xi} = \dot{x}\sin\beta - \dot{y}\cos\beta = \begin{bmatrix}\sin\beta & \cos\beta & 0\end{bmatrix}\begin{bmatrix}\dot{x}\\ \dot{y}\\ \dot{\beta}\end{bmatrix} \tag{2}$$

where β is the yaw angle of the UGV in the inertial coordinate, defined counterclockwise as positive. $\dot{x}$ and $\dot{y}$ are the speeds of the UGV in the inertial coordinate.

One of the necessary and sufficient conditions for a motion constraint to be a non-holonomic constraint is that the accessible distribution dimension i of the system is greater than m (where m is the dimension of ξ minus the number of constraints). From equation (2), $\dot{\xi}$ is in the zero space of the constraint matrix $\Re(\xi)$. The zero space is composed of two column matrices (δ_1 and δ_2) and the relationship is as follows:

$$\begin{bmatrix}\delta_1 & \delta_2\end{bmatrix} = \begin{bmatrix}\cos\beta & 0\\ \sin\beta & 0\\ 0 & 1\end{bmatrix} \tag{3}$$

The dynamic model of the UGV is as follows:

$$\dot{\xi} = \begin{bmatrix}\cos\beta\\ \sin\beta\\ 0\end{bmatrix}u_{linear} + \begin{bmatrix}0\\ 0\\ 1\end{bmatrix}u_{angular} \tag{4}$$

where u_{linear} is the linear velocity control amount and $u_{angular}$ is the angular velocity control amount.

2.2 Kinematic Model Establishment

The kinematic model can reflect the relationship among the current state variables of the UGV and can describe the system model more intuitively. The kinematic model of the UGV is established as follows:

$$\dot{\xi} = \begin{bmatrix}\dot{x}\\ \dot{y}\\ \dot{\beta}\end{bmatrix} = \begin{bmatrix}\frac{r\cos\beta}{2} & \frac{r\cos\beta}{2}\\ \frac{r\sin\beta}{2} & \frac{r\sin\beta}{2}\\ \frac{r}{l} & -\frac{r}{l}\end{bmatrix}\begin{bmatrix}\omega_r\\ \omega_l\end{bmatrix} \tag{5}$$

where ξ is the coordinate vector of the UGV. r is the wheel radius. ω_l and ω_r are the angular velocity of the left and right wheels. l is the distance of the drive wheel.

The established coordinate system is shown in Fig.1.

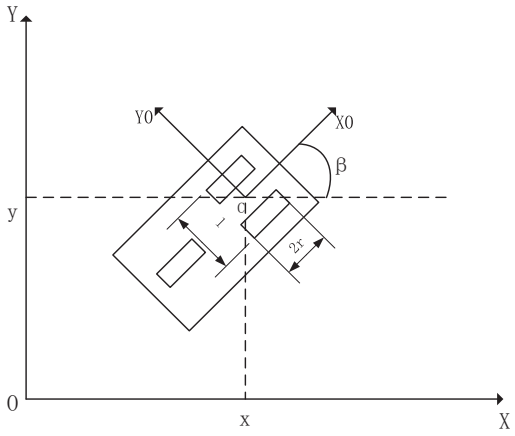

Fig.1: The UGV coordinate system

2.3 Tracking Problem Description

To transform the tracking problem into mathematical problems, a Cartesian coordinate system is established as shown in Fig.2.

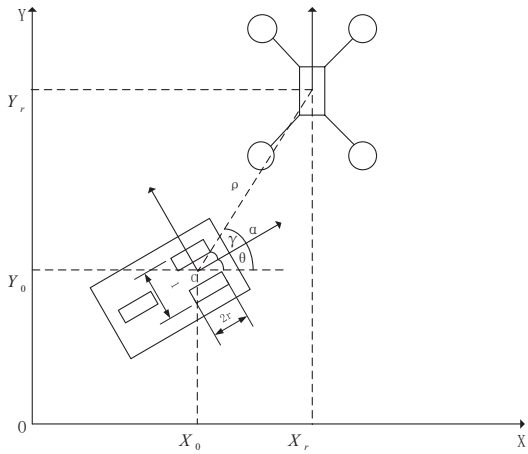

Fig.2: Target tracking schematic diagram

where ρ is the distance between the current position and the target position in the coordinate of the UGV. γ is the angular deviation of the current attitude and the target attitude of the UGV. θ is the angle between the current yaw angle of the UGV and the positive direction of the X-axis in the global coordinate system. α is the angle between the

line from the current position to the target position and the positive direction of the *X*-axis. $q_r = \begin{bmatrix} X_r & Y_r \end{bmatrix}^T$ is the target position in the global coordinate. Assume that the current position of the UGV is $q_0 = \begin{bmatrix} X_0 & Y_0 \end{bmatrix}^T$. Position deviation q_e is as follows:

$$q_e = q_r - q_0 = \begin{bmatrix} X_e \\ Y_e \end{bmatrix} = \begin{bmatrix} X_r - X_0 \\ Y_r - Y_0 \end{bmatrix} \tag{6}$$

The polar coordinate system $\begin{bmatrix} \rho & \gamma \end{bmatrix}^T$ is as follows:

$$\begin{aligned} e_l &= \rho \\ e_a &= \gamma \end{aligned} \tag{7}$$

where e_p is the position deviation and attitude deviation of the UGV in the global coordinate.

$$e_p = \begin{bmatrix} e_l & e_a \end{bmatrix} \tag{8}$$

The position deviation analysis graph is shown in Fig.2. According to the geometric relationship, the position deviation and angle deviation are as follows:

$$e_l = \sqrt{\left(X_e^2 + Y_e^2\right)} \tag{9}$$

$$\alpha = \arctan 2(Y_e, X_e) \tag{10}$$

Finally, the deviation from the current angle to the target point of the UGV is as follows:

$$e_a = \alpha - \theta \tag{11}$$

3 Target Tracking Control Algorithm

Expert PID control belongs to intelligent control, with the characteristics of rapidity, stability and anti-interference. The design of the expert control rules is simpler than other intelligent control algorithms, such as fuzzy control, neural network control and genetic algorithm control. The mathematical model of the expert controller is as follows:

$$U = f\left(E, K, I\right) \tag{12}$$

where f is an intelligent control function, and the basic form is: IF E AND K THEN (IF I THEN U). $E\left\{e_1, e_2, \cdots, e_m\right\}$ is the controller input set, $K\left\{k_1, k_2, \cdots, k_n\right\}$ is the knowledge base, $I\left\{i_1, i_2, \cdots, i_p\right\}$ is inference engine, $U\left\{u_1, u_2, \cdots, u_l\right\}$ is the control output.

According to the knowledge base K, the controller input set E is inferred to determine the parameter adjustment by I and the controller output U is calculated by f.

The core of the expert controller is the knowledge base and the inference engine. According to different functions in the control system, the expert controller is divided into direct type and indirect type. According to the demand, the direct type expert controller is used. In general, the expert knowledge base has only a dozen control rules, which is convenient to modify and transplant. During the parameter adjustment process, the pre-established expert rules are matched, and the parameters of the controller are adjusted. The structure is shown in Fig.3.

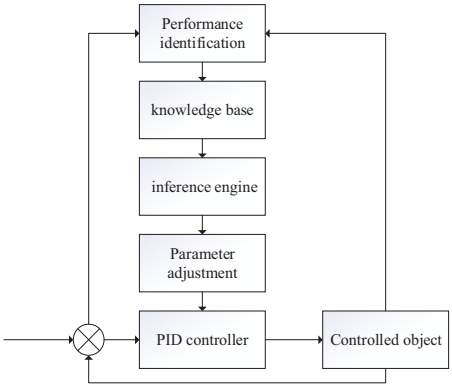

Fig.3: Expert controller composition diagram

First, the motion controller is divided into two channels, namely linear velocity controller and angular velocity controller, which are designed according to equation (8). The linear velocity PID controller uses e_l to generate the control amount. The linear velocity controller is designed as follows:

$$u_{linear} = k_p^l * e_l(t) + k_i^l * \int e_l(t)\,dt + k_d^l * \frac{de_l(t)}{dt} \tag{13}$$

where k_p^l, k_i^l, k_d^l are the parameters of linear controller. The angular velocity PID controller uses e_a to generate the control amount. The angular velocity controller is designed as follows:

$$u_{angular} = k_p^a * e_a(t) + k_i^a * \int e_a(t)\,dt + k_d^a * \frac{de_a(t)}{dt} \tag{14}$$

where k_p^a, k_i^a, k_d^a are the parameters of angular controller. The control amount is passed to the underlying driver, it converts the PID control amount into the desired speed of the two drive wheels. The speed of the drive wheels is measured by the encoder and fed back to the underlying driver. The underlying driver controls the speed of the two drive wheels separately through the underlying PID controller.

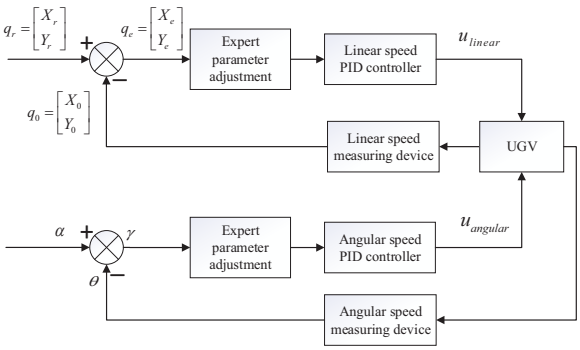

Fig.4: Expert PID control system

When the UAV moves in the direction of the UGV motion constraint, the control amounts of the linear velocity and the angular velocity are simultaneously applied to the underlying driver, and the UGV needs to take a long route to track the UAV. To solve this problem, an expert PID controller is designed. The expert parameters adjustment adjusts the PID parameters according to the knowledge base so that the UGV can correct the angular deviation and

position deviation simultaneously with different response speeds.

In order to build the knowledge base, lots of experiments are carried out. Parameters with different response speed are tuned according to the range of position deviation and angle deviation. The knowledge base is shown in Table 1. The motion constraint must be considered and it has been introduced in 2.2. To solve the problem of sudden change of the control amount during switch parameters, the deviation range is divided and the cubic function fitting smoothing is used. The form of the cubic function is:

$$f(x) = ax^3 + bx^2 + cx + d \tag{15}$$

Adjust the value of a, b, c, d according to the sudden change range of the control amount when switching parameters so that the control amount output smoothly in the form of the cubic function curve. The controller structure of the UGV is shown in Fig.4.

Table 1: Expert PID Knowledge Base

Rules	$e_\alpha >= 120^0$		$60^0 < e_\alpha < 120^0$		$0 \le e_\alpha \le 60^0$	
$e_l \ge 5m$	angular $k_p^a = 0.6$ $k_i^a = 0.0$ $k_d^a = 0.0$	linear $k_p^l = 0.2$ $k_i^l = 0.0$ $k_d^l = 0.0$	angular $k_p^a = 0.4$ $k_i^a = 0.0$ $k_d^a = 0.1$	linear $k_p^l = 0.3$ $k_i^l = 0.0$ $k_d^l = 0.0$	angular $k_p^l = 0.3$ $k_i^l = 0.1$ $k_d^l = 0.08$	linear $k_p^l = 0.4$ $k_i^l = 0.0$ $k_d^l = 0.0$
$3m < e_l < 5m$	angular $k_p^a = 0.6$ $k_i^a = 0.0$ $k_d^a = 0.0$	linear $k_p^l = 0.15$ $k_i^l = 0.0$ $k_d^l = 0.0$	angular $k_p^a = 0.4$ $k_i^a = 0.0$ $k_d^a = 0.1$	linear $k_p^l = 0.18$ $k_i^l = 0.0$ $k_d^l = 0.0$	angular $k_p^l = 0.3$ $k_i^l = 0.1$ $k_d^l = 0.08$	linear $k_p^l = 0.2$ $k_i^l = 0.0$ $k_d^l = 0.0$
$e_l \le 3m$	angular $k_p^a = 0.6$ $k_i^a = 0.0$ $k_d^a = 0.0$	linear $k_p^l = 0.1$ $k_i^l = 0.0$ $k_d^l = 0.0$	angular $k_p^a = 0.4$ $k_i^a = 0.0$ $k_d^a = 0.1$	linear $k_p^l = 0.15$ $k_i^l = 0.0$ $k_d^l = 0.05$	angular $k_p^l = 0.3$ $k_i^l = 0.1$ $k_d^l = 0.08$	linear $k_p^l = 0.18$ $k_i^l = 0.0$ $k_d^l = 0.04$

The expert PID controller can adaptively adjust the parameters when tracking the UAV and select the parameters in Table 1 according to the different e_α and e_l. For example, when $e_\alpha = 160^\circ$ and $e_l = 6m$, the expert parameters adjustment will set the PID parameters to:

$$\begin{cases} k_p^a = 0.6 & k_i^a = 0.0 & k_d^a = 0.0 \\ k_p^l = 0.2 & k_i^l = 0.0 & k_d^l = 0.0 \end{cases} \tag{16}$$

4 Construction of Experiment Platform

4.1 UGV and UAV Construction

According to actual needs, a three-wheeled UGV is used which uses Raspberry Pi as the MCU and STM32F407 as the underlying driver. Meanwhile, PIXHAWK is used as the MCU of the UAV. PIXHAWK and Raspberry Pi can both run Robot operating system (ROS), which makes communication between multiple systems more convenient. To build a hardware communication link, both the UAV and the UGV use RS9113 WIFI modules. This module can provide stable communication in the 5G network environment.

4.2 Motion Capture System

This experimental platform uses the Optitrack system. The advanced real-time Optitrack system is mainly used in indoor environments and GPS inaccessible environments. First of all, the pre-marked markers need to be pasted on the UAV and the UGV. Multiple motion capture cameras are used to detect pre-marked markers. Different arrangement of pre-marked markers can be seen as different rigid bodies. Computing through the Motive software, the accurate position and attitude information of rigid bodies are obtained for the control of the UAV and the UGV.

4.3 Whole Experimental Platform

The experimental platform includes a UGV, a UAV, the Optitrack system and two computers (PC1 and PC2). The PC2 runs the motion control program and sends motion control commands to the UGV and the UAV. The Optitrack system detects markers by motion capture cameras and transmits the data to the PC1. The accurate position and attitude information of the UGV and the UAV are obtained through professional software. The PC1 transmits the information to the PC2 for feedback control. The whole experimental platform is shown in Fig.5.

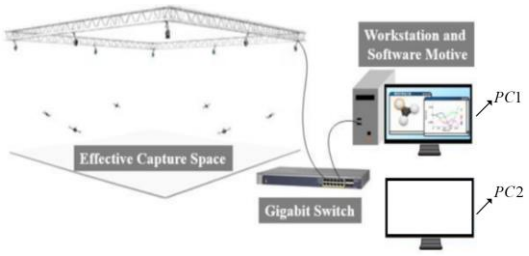

Fig.5: Experimental system structure diagram

5 Experimental Data Analysis

To verify the target tracking effect of the UGV, the UAV only needs to perform simple motion. The UAV achieves corresponding motion by the given points of motion trajectory. To verify the target tracking effect when the UAV moves in the direction of the UAV motion constraint, this experiment allows the UAV to move to the rear of the UGV. Using traditional PID and improved expert PID for comparative experiments, and the experiment process diagram is shown in Fig.6.

Fig.6: The experimental process diagram

Firstly, the UGV uses the traditional PID target tracking control algorithm and the trajectories are shown in Fig.7. Due to the large angle deviation, the UGV needs a large angular velocity control amount to adjust the yaw angle. In the meanwhile, the distance deviation is still large, so that the UGV needs a large linear control amount to adjust position. The actual response result shows that the UGV needs to take a long route to track the UAV. After data calculation, the historical average deviation is 0.11 m, and the overshoot is 0.57 m, and the steady-state deviation between the forward axes of the two vehicles is 0.015 m. The position deviation and speed response are shown in Fig.8. It can be seen that the speed response is relatively smooth, but still has some mutant values. This may lead to unstable movement of the UGV and impact tracking effect.

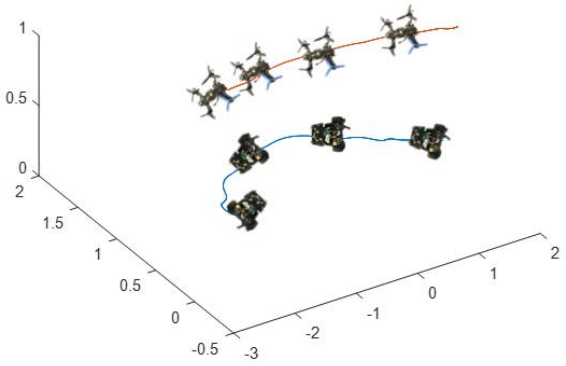

Fig.7: Traditional PID target tracking trajectory

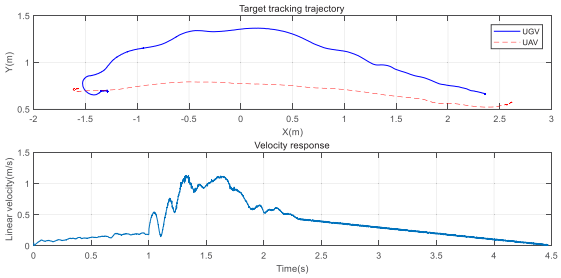

Fig.8: Traditional PID position deviation and speed response

Then, the UGV uses the improved expert PID target control algorithm, and trajectories are shown in Fig.9. From Fig.9, the overshoot is further reduced and the tracking effect is significantly improved. After data calculation, the historical average deviation is 0.04 m, the overshoot is 0.28 m, and the steady-state deviation between the forward axes of the two vehicles is 0.0098 m. The position deviation and speed response are shown in Fig.10. From Fig.10, the speed response is smooth enough to ensure motion stability, and the response has no obvious fluctuation when switching parameters. Although the trajectory of the UAV is slightly different, this experiment mainly verifies the tracking of the UAV when it moves behind the UGV, so these slight differences can be ignored.

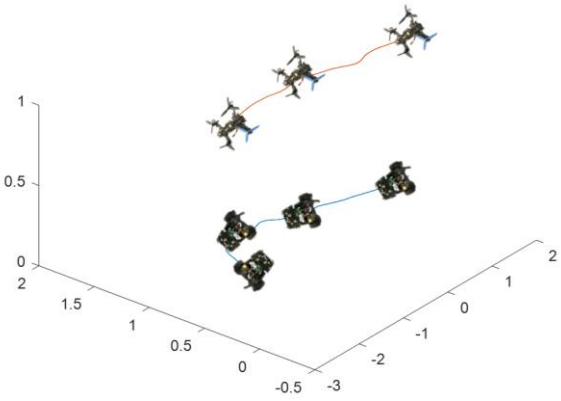

Fig.9: Expert PID target tracking trajectory

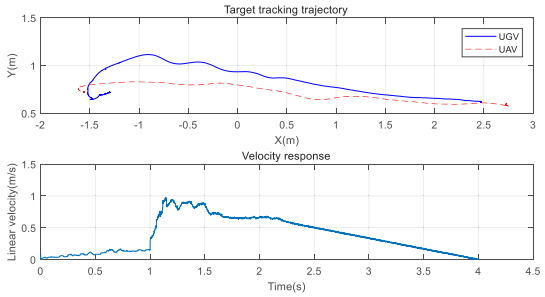

Fig.10: Expert PID position deviation and speed response

In order to verify the response of the proposed target tracking algorithm in the case of ordinary motion, this paper makes the UAV move randomly. From Fig.11, as the UAV moves randomly, the UGV still has an ideal tracking effect. By calculation, the historical average deviation between the forward axes of the two vehicles is 0.13 m.

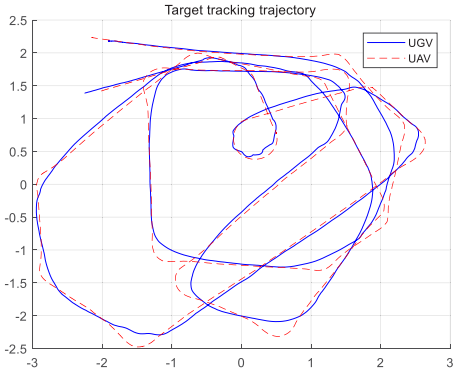

Fig.11: Tracking random motion trajectory

The jitter of the trajectory in Fig.8, Fig.10 and Fig.11 are caused by the unevenness of the field, and the UGV can continue to track the UAV after a short adjustment. It shows that the UGV has satisfactory anti-interference ability and satisfactory tracking effect.

This experiment compares four indicators of historical average deviation, overshoot, steady-state deviation and time cost. The data comparison is shown in Table 2.

Table 2: Comparison of Trajectory Curves

Parameter name	Traditional PID	Expert PID
Historical average deviation	0.11 m	0.04 m
overshoot	0.57 m	0.28 m
Steady-state deviation	0.015 m	0.0098 m
Time cost	4.6 s	4.1 s

6 Conclusion

To solve the problem of the leader-following formation of UAVs and UGVs, the target tracking algorithm of the UGV is improved by combining the idea of expert systems. The PID parameters can be adjusted online according to the knowledge base. It solves the inaccurate tracking cause by fast speed and large angle change when tracking the UAV. In order to build the knowledge base, lots of experiments are carried out. The cubic function fitting smoothing method is used to solve the problem of sudden change of the control amount when switching parameters. This method effectively reduces overshoot and smooths speed response. The improved expert PID target tracking control algorithm is verified by practical experiments.

In the future, the main task is to build a knowledge base acquisition mechanism to improve the knowledge base. Further analysis of the UGV model and consideration of more influencing factors are also needed. The proposed method can be applied to different systems by improving and modifying the knowledge base through the knowledge base acquisition mechanism.

References

[1] Chen J, Zhang X, Xin B, et al. Coordination Between Unmanned Aerial and Ground Vehicles: A Taxonomy and Optimization Perspective. *IEEE Transactions on Cybernetics*, 46(4): 959-972, 2017.

[2] Arbanas, Ivanovic B , Car A , et al. Decentralized planning and control for UAV–UGV cooperative teams, *Autonomous Robots*, 42: 1601-1618, 2018.

[3] Santana L V, Brandao A S, Sarcinelli-Filho M, Heterogeneous leader-follower formation based on kinematic models, *International Conference on Unmanned Aircraft Systems*, 2016: 342-346.

[4] Jiang J, Qi Y, Ibrahim M , et al. Quadrotors' Low-cost Vision-based Autonomous Landing Architecture on a Moving Platform, *15th International Conference on Control, Automation, Robotics and Vision (ICARCV)*, 2018: 448-453.

[5] Chen S, Guo S, Li Y. Real-time tracking a ground moving target in complex indoor and outdoor environments with UAV, *IEEE International Conference on Information and Automation*, 2017: 362-367.

[6] Jin S G, Zhang J Y, Shen L C, Li T X. On-board Vision Autonomous Landing Techniques for Quadrotor: A Survey, *35th Chinese Control Conference*, 2016: 10284-10289.

[7] Yibei L I, Yao Y, Fenghua H E, et al. Autonomous Control and Target Tracking Algorithm Design for A Quadrotor, *China Control Conference*, 2017: 6749-6754.

[8] A Lakas, B Belkhouche, O Benkraouda, A Shuaib, H J Alasmawi, A Framework for a Cooperative UAV-UGV System for Path Discovery and Planning, *2018 International Conference on Innovations in Information Technology (IIT)*, 2018: 42-46.

[9] J Ni, J Hu, C Xiang, Robust Control in Diagonal Move Steer Mode and Experiment on an X-by-Wire UGV, *IEEE/ASME Transactions on Mechatronics*, 42(2): 572-584, 2019.

[10] O Barrero, S Tilaguy, Y M Nova, Outdoors Trajectory Tracking Control for a Four Wheel Skid-Steering Vehicle*, *2018 IEEE 2nd Colombian Conference on Robotics and Automation (CCRA)*, 2018: 1-6.

[11] S Zhu, G Xiong, H Chen, Unmanned Ground Vehicle Control System Design Based on Hybrid Architecture, *2019 IEEE 8th Joint International Information Technology and Artificial Intelligence Conference (ITAIC)*, 2019: 948-951.

[12] Wei W, Tusng-Ming H, Tzu-Sung W, *IEEE 10th International Workshop on Computational Intelligence and Applications*, 2017: 33-38.

[13] Park M W, Lee S W, Han W Y. Development of lateral control system for autonomous vehicle based on adaptive pure pursuit algorithm, *IEEE International Conference on Control, Automation and Systems*, 2014: 1443-1447.

[14] Haytham A, Elhalwagy Y Z, Wassal A, et al. Modeling and simulation of four-wheel steering unmanned ground vehicles using a PID controller, *IEEE International Conference on Engineering and Technology*, 2015: 1-8.

[15] Luo Z, Li W. Tracking of Mobile Robot Expert PID Controller Design and Simulation, *IEEE International Symposium on Computer, Consumer and Control*, 2014: 566-568.